A pH-stabilizing role of voltage-gated proton channels in IgE-mediated activation of human basophils

Boris Musset*†, Deri Morgan*†, Vladimir V. Cherny*, Donald W. MacGlashan, Jr.‡, Larry L. Thomas§, Eduardo Ríos*, and Thomas E. DeCoursey*¶

Departments of *Molecular Biophysics and Physiology and §Immunology/Microbiology, Rush University Medical Center, Chicago, IL 60612; and ‡Johns Hopkins Asthma and Allergy Center, The Johns Hopkins University School of Medicine, Baltimore, MD 21224

Edited by Michael D. Cahalan, University of California, Irvine, CA, and accepted by the Editorial Board May 14, 2008 (received for review January 28, 2008)

Eosinophils and other phagocytes use NADPH oxidase to kill bacteria. Proton channels in human eosinophils and neutrophils are thought to sustain NADPH oxidase activity, and their opening is greatly enhanced by a variety of NADPH oxidase activators, including phorbol myristate acetate (PMA). In nonphagocytic cells that lack NADPH oxidase, no clear effect of PMA on proton channels has been reported. The basophil is a granulocyte that is developmentally closely related to the eosinophil but nevertheless does not express NADPH oxidase. Thus, one might expect that stimulating basophils with PMA would not affect proton currents. However, stimulation of human basophils in perforated-patch configuration with PMA, *N*-formyl-methionyl-leucyl-phenylalanine, or anti-IgE greatly enhanced proton currents, the latter suggesting involvement of proton channels during activation of basophils by allergens through their highly expressed IgE receptor (FcεRI). The anti-IgE-stimulated response occurred in a fraction of cells that varied among donors and was less profound than that to PMA. PKC inhibition reversed the activation of proton channels, and the proton channel response to anti-IgE or PMA persisted in Ca^{2+}-free solutions. Zn^{2+} at concentrations that inhibit proton current inhibited histamine release elicited by PMA or anti-IgE. Studied with confocal microscopy by using SNARF-AM and the shifted excitation and emission ratioing of fluorescence approach, anti-IgE produced acidification that was exacerbated in the presence of 100 μM Zn^{2+}. Evidently, proton channels are active in basophils during IgE-mediated responses and prevent excessive acidification, which may account for their role in histamine release.

asthma | histamine | patch-clamp | HNVCN1 | allergy

The IgE-mediated activation of basophils is a hallmark of allergic reactions. Binding of allergen to allergen-specific IgE on basophils results in cross-linking of high-affinity receptors (FcεRI), thereby activating a signaling pathway that results in the release of histamine and other mediators. Basophils are among several cell types that express voltage-gated proton channels (1). Proton channels are opened by depolarization and/or cytoplasmic acidification and seem to be designed for rapid, efficient acid extrusion from cells (2). In phagocytes, they are thought to enable sustained NADPH oxidase activity by compensating for the electrogenic activity of the oxidase (3–5). Stimuli that activate NADPH oxidase in human eosinophils and neutrophils and in murine osteoclasts greatly enhance the opening of proton channels in these cells studied in perforated-patch configuration (6–10), largely via PKC phosphorylation (11). In contrast, phorbol myristate acetate (PMA) has no clear effect on proton currents in alveolar epithelial cells that lack NADPH oxidase (6). The function of proton channels in basophils is unknown, but must differ from that of phagocytes, because basophils lack NADPH oxidase (12). Here, we show that proton channels in basophils respond vigorously to agents that elicit histamine release. Furthermore, histamine release stimulated by anti-IgE or PMA was inhibited by Zn^{2+} at concentrations that inhibit proton currents, consistent with the idea that proton channel activity is linked to basophil activation. Studies of pH_i using the fluorescent pH sensitive dye SNARF-AM suggest that proton channels limit acidification during basophil responses.

Results

Proton Currents in Human Basophils Respond to PMA. Human basophils voltage-clamped in the perforated-patch configuration exhibit voltage-gated proton currents (Fig. 1*A*) that resemble those in human eosinophils (7), both in properties and in amplitude. In basophils at symmetrical pH 7.0 (50 mM NH_4^+ on both sides of the membrane clamps pH_i near pH_o), the proton conductance, g_H, activates during depolarizing voltage pulses above +20 mV, and activates more rapidly at more positive voltages. The net, leak-subtracted H^+ current (I_H) at +80 mV was 30 ± 18 pA (mean ± SD) in 21 cells. In similar measurements, I_H in human eosinophils was 48 pA (7).

The PKC activator PMA is a potent and effective stimulus of histamine release from basophils (13). Nearly every basophil stimulated with PMA exhibited a profound enhancement of proton currents. After addition of PMA to the bath solution, I_H during a test pulse increased progressively over several minutes (Fig. 1*B*). The same family of pulses in PMA elicited larger currents (Fig. 1*C*) that activated more rapidly at each voltage. H^+ current–voltage relationships (Fig. 1*F*) reveal that the voltage at which the H^+ current was first activated, $V_{threshold}$, was shifted ≈20 mV more negative after stimulation with PMA. The chord conductance (g_H) calculated from the H^+ current (Fig. 1*G*) was also shifted −20 mV by PMA, and the maximum H^+ conductance ($g_{H,max}$) was doubled in this cell. The impression that PMA stimulation increased the opening rate of proton channels is confirmed in Fig. 1*H*. The activation time constant, τ_{act}, was decreased (activation became faster) by ≈3-fold at all voltages. Average responses of proton currents in basophils and neutrophils to PMA are summarized in Table 1. Consistent with the lack of NADPH oxidase (12), no hint of electron current was seen.

The enhanced gating mode, or "activation," of phagocyte proton channels is largely attributable to phosphorylation by PKC of either the channel itself or a closely related protein (11). Fig. 1*D* shows that the PKC inhibitor GF109203X (GFX)

Author contributions: B.M., D.M., V.V.C., D.W.M., L.L.T., E.R., and T.E.D. designed research; B.M., D.M., V.V.C., and D.W.M. performed research; B.M., D.M., V.V.C., D.W.M., L.L.T., E.R., and T.E.D. analyzed data; and D.W.M., L.L.T., and T.E.D. wrote the paper.

The authors declare no conflict of interest.

This article is a PNAS Direct Submission. M.D.C. is a guest editor invited by the Editorial Board.

†B.M., and D.M. contributed equally to this work.

¶To whom correspondence should be addressed. E-mail: tdecours@rush.edu.

This article contains supporting information online at www.pnas.org/cgi/content/full/0800886105/DCSupplemental.

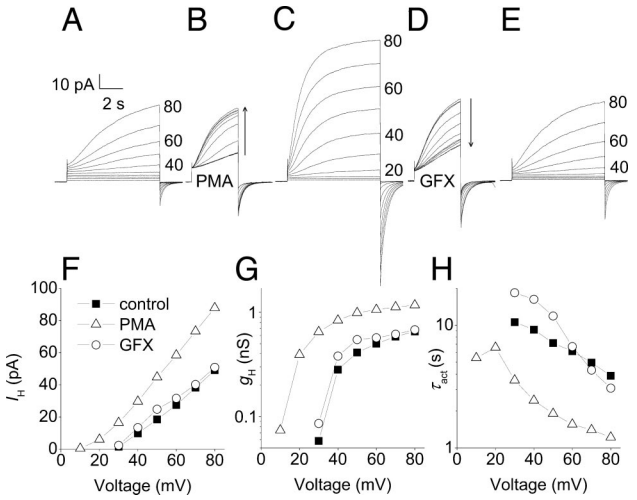

Fig. 1. Proton currents in human basophils respond vigorously to PMA and GFX. (*A*, *C*, and *E*) Families of currents in a basophil before stimulation (*A*), after exposure to 60 nM PMA for 4 min (*C*), and after addition of 2.5 μM GFX (*E*). In each, the membrane was held at −20 mV, and 8-s pulses were applied in 10-mV increments every 30 s up to +80 mV. (*B*) Superimposed currents during the transition to PMA, with 4-s pulses to +60 mV applied every 15 s. (*D*) Test currents after addition of GFX. (*F*) *I–V* relationships from the families in *A*, *C*, and *E*. (*G*) g_H–*V* relationships from the families in *A*, *C*, and *E* were calculated by using V_{rev} measured in each condition and the steady-state I_H obtained by extrapolating exponential fits. (*H*) Voltage dependence of the activation time constant (τ_{act}) obtained by fitting the currents in *A*, *C*, and *E* to a rising exponential (after a delay). Calibration bars apply to *A–E*. The bath included Ca^{2+}.

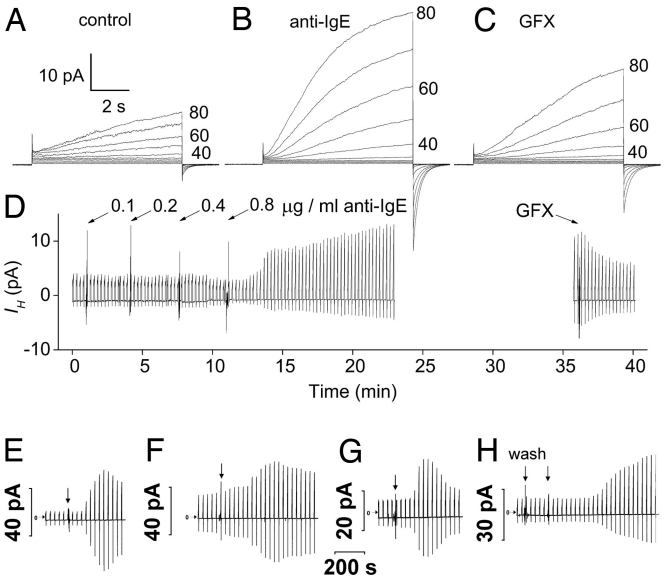

Fig. 2. Proton currents in human basophils are enhanced by anti-IgE stimulation in a GFX-sensitive manner. (*A–C*) Currents in response to the same applied family of pulses before stimulation (*A*), after stimulation by 0.8 μg/ml anti-IgE (*B*), and in the presence of 3 μM GFX (*C*). (*D*) The time course of these responses. Anti-IgE was added to the bath incrementally, and then the bath stirred. The bath was Ca^{2+} free. (*E–H*) Time course of anti-IgE responses in four other basophils. Horizontal arrows indicate zero current. In each, test pulses to +40 mV (*E–G*) or +60 mV (*H*) were applied every 30 s, and at the arrow, 0.6 μg/ml anti-IgE was applied to the bath followed by stirring, except for *G*, where 6.6 μg/ml was applied. In *H*, ''wash'' indicates a bath exchange with the same solution as a control; in this experiment anti-IgE was applied by complete bath exchange. The bath included 2 mM Ca^{2+}, except *H*, which was Ca^{2+}-free.

reversed the increase in I_H produced by PMA in basophils. GFX also reversed the shift in the I_H–*V* relationship (Fig. 1*F*), the increase in $g_{H,max}$ (Fig. 1*G*), and the change in τ_{act} (Fig. 1*H*). In this cell, GFX seemed to reverse all effects of PMA. In contrast, GFX reversed the effects of PMA on proton currents in eosinophils only partially (11).

Proton Currents in Human Basophils Respond to Anti-IgE. The characteristic response of human basophils occurs when allergens bind to IgE, resulting in cross-linking of high-affinity receptors (FcεRI) that activates a signaling pathway that results in the release of histamine and other mediators. Cross-linking IgE with goat anti-human IgE antibody (anti-IgE) elicited a distinct proton channel response (Fig. 2) in a fraction of cells. More than half of the cells from the most responsive donors responded to anti-IgE, but most cells from certain other donors failed to respond. Five cells each from three donors failed to respond to anti-IgE but responded subsequently to PMA. In studies of highly purified (≈98%) basophils (in *Methods*), 60% of cells (6/10) responded to anti-IgE, confirming that some nonresponding cells were basophils. Donor-to-donor variability is typically observed in histamine release by basophils in response to anti-IgE (14, 15).

Table 1. Effects of anti-IgE and PMA on proton currents in human basophils compared with PMA effects in human neutrophils

Parameter	Basophil with anti-IgE	Basophil with PMA	Neutrophil with PMA*
$g_{H,max}$	2.29 ± 0.16 (31) (anti-IgE/control)	2.86 ± 0.21 (40) (PMA/control)	1.9 (PMA/control)
τ_{act} at V_{test}	2.17 ± 0.19 (28) (control/anti-IgE)	5.04 ± 0.56 (52) (control/PMA)	3.7 (control/PMA)
τ_{tail} at V_{hold}	1.20 ± 0.04 (33) (anti-IgE/control)	1.32 ± 0.07 (64) (PMA/control)	5.5 (PMA/control)
$\Delta V_{threshold}$, mV	−11.0 ± 0.9 (33) (anti-IgE − control)	−19.0 ± 1.0 (61) (PMA − control)	−38.8 (PMA − control)

Parameters [mean ± SEM (*n*)] were measured when the effects of PMA (60–160 nM) or anti-IgE (usually 0.5–1.0 μg/ml) peaked or approached steady state, usually within a few minutes. Only cells that clearly responded are included. Responses are given as ratios where 1.0 means no response, except for $V_{threshold}$, for which 0 mV means no response. The $g_{H,max}$ values were calculated from the largest pulses applied. Gating kinetics, τ_{act} and τ_{tail}, respectively, were obtained from exponential fits to currents during test pulses or upon repolarization to the holding potential (V_{hold}). Data for Ca^{2+} or Ca^{2+}-free bath are combined because no parameter differed significantly for either stimulus. All PMA effects except on τ_{tail} are significantly greater ($P < 0.05$) than those for anti-IgE. *Values from a previous study (6).

Anti-IgE responses in Fig. 2 *D–H* illustrate the variety of time courses observed. Depolarizing pulses were applied every 30 s to elicit proton currents. Typically, there was a delay of 1 min to several minutes before the onset of a response. I_H then began to increase. In some cells, I_H peaked and immediately began to decline (Fig. 2 *E* and *G*), although not to its original amplitude. In other cells, I_H remained elevated for prolonged periods. These responses were observed after stimulation with anti-IgE at concentrations ranging from 0.2 to 10 μg/ml. At higher concentrations, the response seemed more rapid and transient, but there were exceptions. Most measurements were performed by using 0.5–1.0 μg/ml anti-IgE.

In the experiment in Fig. 2*D*, anti-IgE was added incrementally, with a profound response occurring at 0.8 μg/ml. In families of currents recorded before and after the addition of anti-IgE (Fig. 2 *A* and *B*), the H^+ current was larger and activated faster at each voltage after anti-IgE. In Table 1, the parameter values during the peak of the anti-IgE response are given. In cells responding to anti-IgE, $g_{H,max}$ doubled, and channel opening was faster (smaller τ_{act}), but closing kinetics (τ_{tail}) was not affected. The proton conductance–voltage (g_H–V) relationship characterized as $V_{threshold}$ was shifted −11 mV by anti-IgE and −20 mV by PMA. Proton channel responses to anti-IgE and PMA in human basophils were qualitatively identical, but the anti-IgE responses were consistently smaller.

In basophils that exhibited a sustained increase in proton current in response to anti-IgE, GFX reversed the anti-IgE effects distinctly but not completely (Fig. 2 *C* and *D*). In cells that responded to anti-IgE with a transient increase in I_H (e.g., Fig. 2*G*), GFX added after the response had subsided but remained above the initial level, further reduced the current (data not shown).

Roughly half the cells studied did not respond to anti-IgE but did respond to a subsequent application of PMA, confirming that they had not entered whole-cell configuration due to spontaneous patch rupture, which abolishes the PMA response in eosinophils (16). Addition of PMA to cells that had already responded to anti-IgE invariably produced a greater response that (compared with their initial state) was indistinguishable from the response of cells stimulated only with PMA (Table 1 and not shown). GFX reversed most of the combined effects of anti-IgE and PMA (data not shown).

fMLF Also Activates Proton Channels. Stimulation of basophils with 10 μM *N*-formyl-methionyl-leucyl-phenylalanine (fMLF), another agonist of histamine release (15), enhanced proton currents in 10 of 23 cells studied (data not shown). The response to fMLF resembled that to anti-IgE and was augmented by subsequent addition of PMA ($n = 8$). GFX partially reversed the effect of fMLF alone ($n = 1$) or fMLF and PMA together ($n = 4$).

Proton Channel Responses Do Not Require Ca^{2+} Influx. Basophil proton channels responded to PMA or anti-IgE whether or not Ca^{2+} was present in the bath. Considering only cells from two responsive donors, 14 of 22 cells (64%) responded to anti-IgE with ≈0.5 mM free Ca^{2+} (1.5 mM $CaCl_2$ and 1 mM EGTA) in the bath, and 13 of 20 cells (65%) responded to anti-IgE in a Ca^{2+}-free (EGTA-containing) bath solution. The presence or absence of Ca^{2+} in the bath did not detectably affect the magnitude of any proton channel response to PMA or anti-IgE [supporting information Tables S1 and S2]. Proton channels in basophils exposed to 20 μM 1,2-bis(2-aminophenoxy)ethane-N,N,N′,N′-tetraacetic acid, tetraacetoxymethyl ester (BAPTA-AM) in Ca^{2+}-free solutions responded to stimulation with anti-IgE ($n = 3$) or PMA ($n = 2$), suggesting that elevated $[Ca^{2+}]_i$ is not required for a response.

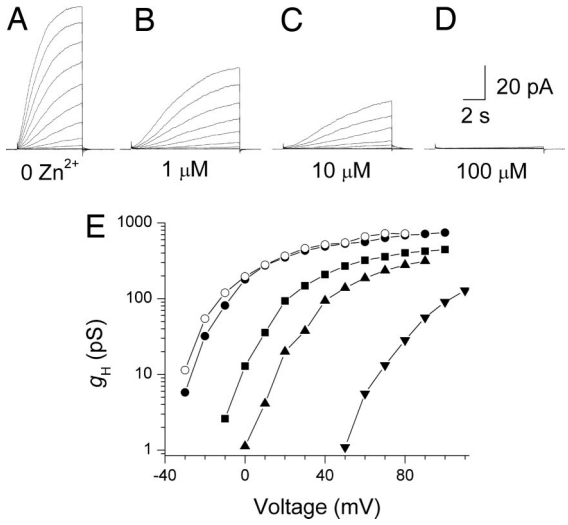

Fig. 3. Effects of Zn^{2+} on proton currents in a human basophil at pH_o 7.4 (Ringer's solution without EGTA) and pH_i 5.5. (*A–D*) Families of currents in response to depolarizing pulses applied from a holding potential of −60 mV to +60 mV in 10-mV increments. The Zn^{2+} concentration was 0 (*A*), 1 μM (*B*), 10 μM (*C*), and 100 μM (*D*). (*E*) The g_H–V relationships from this experiment, calculated by using the current at the end of 6-s pulses (control and wash) or 10-s pulses (all Zn^{2+} concentrations). Symbols in the order of the experiment are ● (control), ■ (1 μM Zn^{2+}), ▲ (10 μM Zn^{2+}), ▼ (100 μM Zn^{2+}), and ○ (after washout). Because Zn^{2+} slows activation, the current amplitude at the end of the pulse increasingly underestimates the steady-state value at higher $[Zn^{2+}]$. Pulses to larger voltages are included in *E*.

Proton Channel Response Precedes Degranulation. If histamine storage granules expressed proton channels, their fusion with the plasma membrane might increase g_H owing to channel insertion. However, the capacitance of a sample of basophils did not change significantly after proton channel responses to anti-IgE (mean ± SE increase 10 ± 9%, $n = 16$) or PMA (mean decrease 6 ± 11%, $n = 10$). Histamine release is slow, especially with PMA as a stimulus (17) and likely did not occur during the proton channel response.

Zinc Inhibition of Proton Currents in Human Basophils. Typically, voltage-gated proton currents are inhibited potently by Zn^{2+} and other polyvalent metal cations, but Zn^{2+} sensitivity of proton currents in basophils has not been reported. Fig. 3 illustrates the effects of Zn^{2+} on proton currents in a human basophil. Currents during pulses in 10-mV increments up to +60 mV are shown for a basophil in whole-cell configuration in the absence of Zn^{2+} and in the presence of 1, 10, and 100 μM Zn^{2+}. As in other cells (2), Zn^{2+} slowed the activation of H^+ current at each voltage and shifted the g_H–V relationship positively (Fig. 3*E*). Zn^{2+} seems to reduce $g_{H,max}$, but g_H was calculated from I_H at the end of 6- to 10-s pulses. Because Zn^{2+} slows activation, I_H at the end of the pulse increasingly underestimates the steady-state value at higher $[Zn^{2+}]$. The shift of the g_H–V relationship, estimated at ≈10% of $g_{H,max}$, was 27 ± 4 mV (mean ± SEM, $n = 5$) at 1 μM Zn^{2+}, 51 ± 8 mV ($n = 5$) at 10 μM Zn^{2+}, and 106 ± 7 mV ($n = 3$) at 100 μM Zn^{2+}. These shifts are close to the expectation of Zn^{2+} effects at pH 7.4 in rat alveolar epithelial cells, where analogous data exist (18), suggesting similar affinity of Zn^{2+} for H^+ channels in both cells.

The potency of Zn^{2+} in inhibiting proton currents in basophils activated with PMA in perforated-patch configuration was also examined. A previous study reported that Zn^{2+} inhibited proton current in activated eosinophils with 20-fold greater potency than in unstimulated cells (5), although this conclusion likely reflected the experimental design rather than a genuine difference in efficacy (7). By the same type of analysis performed for

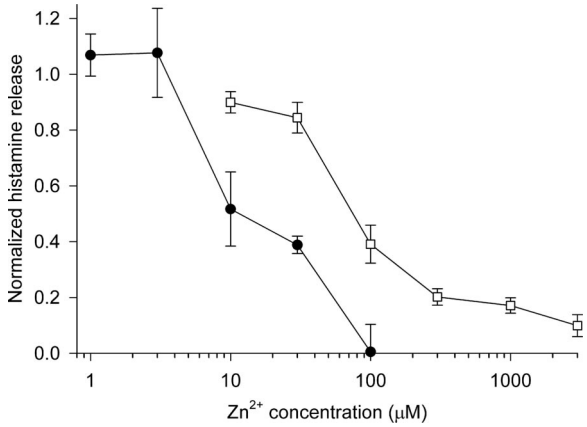

Fig. 4. Inhibition of histamine release by Zn^{2+}. Histamine release induced by 0.3 μg/ml anti-IgE (●) or 60 nM PMA (□) in the presence of various concentrations of $ZnCl_2$, normalized to release in the absence of $ZnCl_2$. Each value is the mean ± SEM of measurements in three to five experiments using blood from different donors. Spontaneous release was 10.0 ± 0.9% (mean ± SEM, $n = 5$) of total histamine content (range 7.7–12.9%), the PMA stimulated release was 65 ± 7% (42–82%, $n = 5$ except $n = 3$ at 10 μM Zn^{2+}), and the anti-IgE stimulated release was 24 ± 6% (13–34%, $n = 3$). The values for the two stimuli at 30 μM and 100 μM differ significantly ($P < 0.001$ and $P < 0.05$, respectively, by Student's t test).

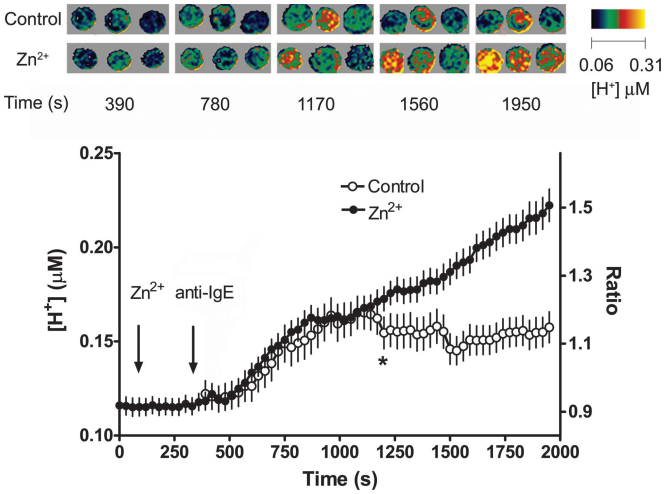

Fig. 5. Average $[H^+]_i$ in basophils (99% pure) stimulated with 1 μg/ml anti-IgE in the absence (○) or presence of 100 μM Zn^{2+} (●) at ≈30°C and imaged by using confocal microscopy and SEER. The mean ± SEM of 25 control cells and 46 cells in Zn^{2+} is shown, with all data pairs after the star significantly different by Student's t test ($P < 0.05$). Pseudocolor images indicating $[H^+]_i$ in trios of basophils from this experiment taken after stimulation with anti-IgE at the indicated time points are shown in two rows; the top row is control, the lower in the presence of Zn^{2+}.

whole-cell studies, the Zn^{2+} sensitivity was similar in basophils studied in perforated-patch configuration after PMA stimulation. The average shift of the g_H–V relationship was 25 ± 6 mV ($n = 4$) at 1 μM Zn^{2+}, 45 ± 4 mV ($n = 5$) at 10 μM Zn^{2+}, and 67 ± 8 mV ($n = 3$) at 100 μM Zn^{2+}. The slightly lower efficacy in these measurements may reflect the lower pH_o of 7.0 compared with pH_o 7.4 for the whole-cells studies. Competition between H^+ and Zn^{2+} reduces the apparent potency of Zn^{2+} at lower pH_o (18). Thus, the affinity of externally applied Zn^{2+} for proton channels in basophils is similar before or after stimulation.

Histamine Release Is Inhibited by Zn^{2+}. To explore whether proton channel activity is involved in basophil function, we measured histamine release in the presence of the proton channel inhibitor, Zn^{2+}. Zn^{2+} inhibits histamine release stimulated by several agonists (19), but PMA stimulation had not been explored. Fig. 4 shows that Zn^{2+} inhibited histamine release elicited by anti-IgE (●) or by PMA (□). Inhibition was more potent with anti-IgE as a stimulus ($IC_{50} \approx 20$ μM) than with PMA ($IC_{50} \approx 90$ μM). Zn^{2+} also inhibited histamine release in basophils stimulated with PMA in a nominally Ca^{2+}-free solution (1 mM Mg^{2+} and no added Ca^{2+}), by 76 ± 12% ($n = 3$) at 100 μM Zn^{2+}.

Proton Channels Extrude Acid Generated During the Anti-IgE Response. If proton channels are active in stimulated basophils, Zn^{2+} should prevent acid extrusion. Fig. 5 shows the anti-IgE response of several basophils examined by fluorescence imaging using confocal microscopy with SNARF labeling and the shifted excitation and emission ratioing of fluorescence (SEER) method (20). The graph shows the average time course of $[H^+]_i$ in many individual cells. In Ringer's solution, anti-IgE resulted in acidification (○) that was more profound in the presence of 100 μM Zn^{2+} (●). Zn^{2+} had no consistent acute effect on unstimulated cells. In 5 other experiments at temperatures ranging from 20°C to 30°C, anti-IgE produced greater acidification with less tendency to recover in the presence of Zn^{2+}. Evidently, a Zn^{2+} sensitive proton extrusion mechanism in the plasma membrane is active during IgE-mediated responses.

Discussion

Proton Currents in Human Basophils Are Enhanced by PMA, Anti-IgE, and fMLF. Proton channel gating in human basophils was enhanced profoundly by PMA stimulation. As occurs in neutrophils (6), PLB-985 cells (8), and eosinophils (5, 7), I_H and $g_{H,max}$ increased, τ_{act} decreased, and $V_{threshold}$ was shifted negatively (Table 1). All of these changes tend to increase proton current at any given voltage. Although other changes were generally similar, the shift in $V_{threshold}$ was only half as large in basophils as in human neutrophils studied under identical conditions, −20 mV compared with −39 mV, respectively, and there was no clear slowing of τ_{tail} in basophils, in contrast to the dramatic slowing seen in neutrophils and other phagocytes. The response pattern of basophils is strikingly reminiscent of that in phagocytes that lack $gp91^{phox}$ expression, including cells from chronic granulomatous disease patients and $gp91^{phox}$ knockout PLB-985 cells (8). In contrast, PMA has no clear effect on proton currents in rat alveolar epithelial cells (6) or in HEK-293 or COS-7 cells transfected with the human or mouse proton channel gene (21). There appears to be a full response in phagocytes (neutrophils, PLB-985 cells, and eosinophils), a partial response in leukocytes (including basophils) lacking NADPH oxidase, and little or no response in other cells. Perhaps this is coincidental, but the pattern is striking nonetheless.

Proton current responses in human basophils speak against the hypothesis that the $gp91^{phox}$ component of NADPH oxidase is a functioning proton channel (5, 22). That large proton currents are present in basophils (1) that lack detectable cytochrome b_{558}, which contains $gp91^{phox}$ (12) establishes that $gp91^{phox}$ is not the proton channel in unstimulated basophils. In the present study, we show that PMA increased $g_{H,max}$ as much in basophils that lack $gp91^{phox}$ as it did in eosinophils and neutrophils with ample $gp91^{phox}$. Therefore, the enhanced proton conductance in phagocytes does not reflect the activity of $gp91^{phox}$.

More surprising than the PMA response was the finding that stimulation of basophils through receptor-mediated pathways by anti-IgE or fMLF also enhanced proton currents. Qualitatively, the anti-IgE response was identical to that elicited by PMA, but it was less profound and was often not sustained. In cells with a

clear anti-IgE response, subsequent addition of PMA invariably produced an augmented response. There are striking similarities between the stimulation of proton channels and histamine release from basophils. There was marked variability among donors in the responsiveness of their basophils to anti-IgE, with proton channel response rates ranging from 0 to 69%. Nearly all cells from all donors responded to PMA. Donor-to-donor variability in histamine release in response to anti-IgE (14, 15) mirrors the variability in proton channel responsiveness. In the general population, the distribution of responsiveness of basophils to activation by anti-IgE is broad, ranging 100-fold, but basophils respond well to PMA even in individuals whose basophil response to anti-IgE is not detectable (14). In addition, the proton channel response occurred after a delay reminiscent of the distinct delay that precedes the increase in $[Ca^{2+}]_i$ (23, 24) and the release of histamine in basophils stimulated with anti-IgE (17) or ragweed pollen antigen (25).

Pathways That Activate Histamine Release and Proton Channels in Basophils Are Not Identical and Vary According to Agonist. Histamine release from basophils elicited by PMA is inhibited by the selective PKC inhibitor GFX. In contrast, anti-IgE stimulated histamine release is insensitive to GFX, and inhibition by several other PKC inhibitors is attributable to their effects on other kinases (15, 26). PKC activity has been implicated in both activating and de-activating signaling in both rat basophilic leukemia cells and human basophils. Therefore, inhibitors of the broader family of PKC isozymes might produce a weak effect on secretion, due to competing inhibition of both activating and de-activating mechanisms. GFX reversed the activation of proton channels by PMA or anti-IgE, supporting a role for phosphorylation in proton channel activation by either agonist. The anti-IgE response was only partially reversed, suggesting involvement of an additional pathway. The lack of capacitance changes during proton channel responses together with previous studies of the time course of histamine release (17) indicate that proton channel enhancement likely precedes degranulation.

The proton channel inhibitors Zn^{2+} and La^{3+} inhibit histamine release from basophils stimulated with anti-IgE or A23187 (19, 27), raising the possibility that proton channels are involved. However, both metal cations also inhibit calcium release activated calcium (CRAC) currents (28) and Na^+/Ca^{2+} exchange (29). Hypothetically, either transporter, if present in basophils, might mediate the Ca^{2+} influx that is required for histamine release in response to anti-IgE (30). Although CRAC currents have not been recorded in basophils, they exist in human neutrophils (31), and CRACM1 protein is expressed in basophils (D.W.M., unpublished data). However, Zn^{2+} inhibits histamine release from rat basophilic leukemia cells more potently than it prevents Ca^{2+} influx, suggesting that it acts by a different mechanism (32). Surprisingly, Ca^{2+} influx stimulated by anti-IgE in human basophils was not inhibited by up to 300 μM Zn^{2+} (D.W.M., unpublished data). This result suggests that in human basophils, CRAC channels either have low Zn^{2+} sensitivity, or they do not mediate the anti-IgE induced Ca^{2+} influx required for histamine release.

To isolate proton channel involvement in histamine release, we examined the Zn^{2+} sensitivity of histamine release induced by PMA, which occurs without Ca^{2+} influx (13) or $[Ca^{2+}]_i$ increases (26, 33); in fact, PMA inhibits CRAC currents (34). The proton channel responses to either PMA or anti-IgE occurred in Ca^{2+}-free solutions and were indistinguishable from responses in Ca^{2+}-containing solutions and hence are independent of Ca^{2+} influx. That histamine release stimulated by PMA was inhibited by Zn^{2+} (Fig. 4) suggests that proton channel activity may be required. The inhibition by Zn^{2+} seemed to be more potent for anti-IgE ($IC_{50} \approx 20$ μM) than for PMA-stimulated ($IC_{50} \approx 90$ μM) responses, consistent with a previous study in which histamine release elicited by anti-IgE and fMLF was inhibited by Zn^{2+}, with IC_{50} 10 μM and 40 μM, respectively (19). The variable sensitivity to Zn^{2+} was attributed to each agonist activating histamine release by a different mechanism. Because the anti-IgE response requires Ca^{2+} influx, but the responses to fMLF and PMA do not (30, 33), the anti-IgE response might normally involve a combination of proton channels and CRAC channels (or whatever mediates Ca^{2+} influx), whereas the PMA and fMLF responses may reflect Zn^{2+} acting exclusively on proton channels.

The Zn^{2+} data suggest that proton channels are required for histamine release. Proton channels might facilitate histamine release by compensating charge, as they do in phagocytes (3, 4), or by modulating pH. Outward H^+ current could compensate for electrogenic Ca^{2+} influx, which is required for anti-IgE-stimulated histamine release. However, during the PMA response, which does not involve Ca^{2+} influx, proton channels must act by a different mechanism. Histamine release consumes metabolic energy (13, 25, 27) and thus likely generates cytoplasmic acid. Consistent with this interpretation, the results in Fig. 5 showed acidification after anti-IgE stimulation, which has not been reported previously. Importantly, Zn^{2+} unmasked occult proton efflux during the response, thereby indicating that proton channels are most likely responsible. Other plasma membrane proton extrusion mechanisms (Na^+/H^+-antiport and H^+-ATPase) are insensitive to Zn^{2+} (35, 36). Together, these results indicate that voltage-gated proton channels in basophils may help keep pH_i in an optimal range for histamine secretion.

Methods

Isolation of Human Basophils. Basophil-containing mononuclear cell fractions were isolated by density gradient centrifugation from freshly drawn venous blood of healthy adult donors according to a protocol approved by the Institutional Review Board of Rush University Medical Center. Basophils were enriched by negative selection using immunomagnetic beads (Basophil Isolation Kit; Miltenyi Biotec, Auburn, CA) and the miniMacs magnetic cell separation system (Miltenyi Biotec) according to the manufacturer's instructions; cells enriched by this method are 59–88% basophils (37). For some experiments basophils were further purified by countercurrent elutriation and two-step Percoll density gradient followed by negative selection (24), resulting in 98–99% purity by Alcian blue staining. The basophils were suspended in PBS with 2 mM EDTA and 0.5% BSA. Freshly isolated cells and cells maintained for up to 2 days at 4°C were used for electrophysiologic measurements.

Electrophysiology. Standard whole-cell or perforated-patch recording was performed as described previously (16). Spherical, nonadherent cells 7–8 μm in diameter (1.68 ± 0.49 pF, mean ± SD, $n = 147$) were selected. Seals were formed with Ringer's solution (in mM: 160 NaCl, 4.5 KCl, 2 $CaCl_2$, 1 $MgCl_2$, 5 Hepes, pH 7.4) in the bath, and the potential zeroed after the pipette was in contact with the cell. For perforated-patch recording, the pipette and bath solutions contained 110 mM tetramethylammonium methanesulfonate, 50 mM NH_4^+ in the form of 25 mM $(NH_4)_2SO_4$, 2 mM $MgCl_2$, 10 mM BES buffer, and 1 mM EGTA and were titrated to pH 7.0 with tetramethylammonium hydroxide. A Ca^{2+}-containing bath solution was identical, but with 1.5 mM $CaCl_2$ added. The NH_4^+ in bath and pipette solutions "clamps" pH_i near pH_o (6, 38). The pipette solution included ≈500 μg/ml solubilized amphotericin B (≈45% purity; Sigma); the pipette tip was dipped briefly into amphotericin-free solution. For whole-cell recording, bath and pipette solutions contained 100–200 mM buffer, 1–2 mM $CaCl_2$ or $MgCl_2$ (pipette solutions were Ca-free), 1–2 mM EGTA, and $TMAMeSO_3$ to adjust the osmolality to ≈300 mOsm, titrated with tetramethylammonium hydroxide or methanesulfonate. No liquid junction potential or leak correction has been applied. Experiments were performed at room temperature (20–25°C). Bioactive substances (PMA, anti-IgE, or GFX) were introduced by complete bath changes or were added directly to the bath with subsequent stirring. Nominal concentrations were calculated according to approximate bath volume, and stirring may not have always been complete; thus, stated concentrations are somewhat approximate. Basophils were stimulated with affinity purified goat anti-human IgE (Immunology Consultants Laboratory).

Histamine Release. Basophil-containing mononuclear cell fractions were isolated from venous blood of healthy adult donors as described above. The cells

were suspended in Ringer containing 5 mM glucose, and 0.003% BSA was added directly to each sample before incubation. Contaminating metals in Millipore purified water had been removedby using Chelex 100 Resin (Bio-Rad Laboratories) before adding salts and glucose. The cells (20,000–45,000 basophils as determined by Alcian blue staining) were incubated with the indicated concentrations of anti-IgE or PMA alone and in the presence of the indicated concentrations of $ZnCl_2$ for 45–60 min at 37°C in round-bottom polystyrene tubes. Total incubation volume was 1 ml. Reactions were stopped by ice. After centrifugation, histamine content in the supernatants was measured by an automated fluorometric assay (39). Spontaneous histamine release was measured by using cells incubated in the absence of stimulus. Total histamine content was measured in supernatants of cells lysed with 1.4% perchloric acid. Results are expressed as histamine released above the spontaneous value.

Dynamic Imaging of the Cytosolic pH of Individual Basophils by SEER Imaging. Human basophils were allowed to adhere to glass coverslips, incubated with 10 μM 5-(and 6-)carboxy SNARF-1 in HBSS for 15–20 min at room temperature, and washed. SEER imaging (20) was performed by simultaneously acquiring 2 confocal images: F_1, excited at 514 nm and emitted at 500–604 nm and F_2 (excited at 594 nm and emitted at 620–715 nm). The ratio F_1/F_2 monitors $[H^+]$ with a dynamic range of $\approx$150.

ACKNOWLEDGMENTS. We thank Dr. Tatiana Iastrebova for excellent technical assistance. This work was supported by the Schmidtmann Foundation (B.M.); National Institutes of Health Heart, Lung and Blood Institute Research Grant HL61437 (to T.D.); and by Philip Morris, USA and Philip Morris International (T.D.).

1. Cherny VV, Thomas LL, DeCoursey TE (2001) Voltage-gated proton currents in human basophils. *Biol Membr* 18:458–465.
2. DeCoursey TE (2003) Voltage-gated proton channels and other proton transfer pathways. *Physiol Rev* 83:475–579.
3. Henderson LM, Chappell JB, Jones OTG (1987) The superoxide-generating NADPH oxidase of human neutrophils is electrogenic and associated with an H^+ channel. *Biochem J* 246:325–329.
4. DeCoursey TE, Morgan D, Cherny VV (2003) The voltage dependence of NADPH oxidase reveals why phagocytes need proton channels. *Nature* 422:531–534.
5. Bánfi B, *et al*. (1999) A novel H^+ conductance in eosinophils: Unique characteristics and absence in chronic granulomatous disease. *J Exp Med* 190:183–194.
6. DeCoursey TE, Cherny VV, Zhou W, Thomas LL (2000) Simultaneous activation of NADPH oxidase-related proton and electron currents in human neutrophils. *Proc Natl Acad Sci USA* 97:6885–6889.
7. DeCoursey TE, Cherny VV, DeCoursey AG, Xu W, Thomas LL (2001) Interactions between NADPH oxidase-related proton and electron currents in human eosinophils. *J Physiol* 535:767–781.
8. DeCoursey TE, Cherny VV, Morgan D, Katz BZ, Dinauer MC (2001) The $gp91^{phox}$ component of NADPH oxidase is not the voltage-gated proton channel in phagocytes, but it helps. *J Biol Chem* 276:36063–36066.
9. Cherny VV, Henderson LM, Xu W, Thomas LL, DeCoursey TE (2001) Activation of NADPH oxidase-related proton and electron currents in human eosinophils by arachidonic acid. *J Physiol* 535:783–794.
10. Mori H, *et al*. (2003) Regulatory mechanisms and physiological relevance of a voltage-gated H^+ channel in murine osteoclasts: Phorbol myristate acetate induces cell acidosis and the channel activation. *J Bone Miner Res* 18:2069–2076.
11. Morgan D, *et al*. (2007) Sustained activation of proton channels and NADPH oxidase in human eosinophils and murine granulocytes requires PKC but not $cPLA_2\alpha$ activity. *J Physiol* 579:327–344.
12. de Boer M, Roos D (1986) Metabolic comparison between basophils and other leukocytes from human blood. *J Immunol* 136:3447–3454.
13. Schleimer RP, Gillespie E, Lichtenstein LM (1981) Release of histamine from human leukocytes stimulated with the tumor-promoting phorbol diesters. I. Characterization of the response. *J Immunol* 126:570–574.
14. Nguyen KL, Gillis S, MacGlashan DW, Jr (1990) A comparative study of releasing and nonreleasing human basophils: Nonreleasing basophils lack an early component of the signal transduction pathway that follows IgE cross-linking. *J Allergy Clin Immunol* 85:1020–1029.
15. Knol EF, Koenderman L, Mul FP, Verhoeven AJ, Roos D (1990) Differential mechanisms in the stimulus-secretion coupling in human basophils: Evidence for a protein-kinase-C-dependent and a protein-kinase-C-independent route. *Agents Actions* 30:49–52.
16. Morgan D, *et al*. (2003) Temperature dependence of NADPH oxidase in human eosinophils. *J Physiol* 550:447–458.
17. Knol EF, Koenderman L, Mul FP, Verhoeven AJ, Roos D (1991) Differential activation of human basophils by anti-IgE and formyl-methionyl-leucyl-phenylalanine. Indications for protein kinase C-dependent and -independent activation pathways. *Eur J Immunol* 21:881–885.
18. Cherny VV, DeCoursey TE (1999) pH-dependent inhibition of voltage-gated H^+ currents in rat alveolar epithelial cells by Zn^{2+} and other divalent cations. *J Gen Physiol* 114:819–838.
19. Marone G, Findlay SR, Lichtenstein LM (1981) Modulation of histamine release from human basophils *in vitro* by physiological concentrations of zinc. *J Pharmacol Exp Ther* 217:292–298.
20. Launikonis BS, Zhou J, Royer L, Shannon TR, Brum G, Ríos E (2005) Confocal imaging of $[Ca^{2+}]$ in cellular organelles by SEER, shifted excitation and emission ratioing of fluorescence. *J Physiol* 567:523–543.
21. Musset B, *et al.* (2008) Detailed comparison of expressed and native voltage-gated proton channel currents. *J Physiol* 586:2477–2486.
22. Henderson LM, Banting G, Chappell JB (1995) The arachidonate-activatable, NADPH oxidase-associated H^+ channel. Evidence that gp91-*phox* functions as an essential part of the channel. *J Biol Chem* 270:5909–5916.
23. MacGlashan DW, Jr, Gleich GJ, Thomas LL (1997) Increases in cytosolic Ca^{2+} accompany basophil activation by eosinophil granule major basic protein. *Immunol Lett* 58:37–42.
24. MacGlashan D, Jr, Lavens-Phillips S (2001) Characteristics of the free cytosolic calcium timelag following IgE-mediated stimulation of human basophils: Significance for the nonreleasing basophil phenotype. *J Leukoc Biol* 69:224–232.
25. Lichtenstein LM, Osler AG (1964) Studies on the mechanisms of hypersensitivity phenomena. IX. Histamine release from human leukocytes by ragweed pollen antigen. *J Exp Med* 120:507–530.
26. Miura K, MacGlashan DW, Jr (1998) Expression of protein kinase C isozymes in human basophils: Regulation by physiological and nonphysiological stimuli. *Blood* 92:1206–1218.
27. Lichtenstein LM (1975) The mechanism of basophil histamine release induced by antigen and by the calcium ionophore A23187. *J Immunol* 114:1692–1699.
28. Zhang L, McCloskey MA (1995) Immunoglobulin E receptor-activated calcium conductance in rat mast cells. *J Physiol* 483:59–66.
29. Simchowitz L, Foy MA, Cragoe EJ (1990) A role for Na^+/Ca^{2+} exchange in the generation of superoxide radicals by human neutrophils. *J Biol Chem* 265:13449–13456.
30. MacGlashan D, Jr, Botana LM (1993) Biphasic Ca^{2+} responses in human basophils. Evidence that the initial transient elevation associated with the mobilization of intracellular calcium is an insufficient signal for degranulation. *J Immunol* 150:980–991.
31. Demaurex N, Monod A, Lew DP, Krause K-H (1994) Characterization of receptor-mediated and store-regulated Ca^{2+} influx in human neutrophils. *Biochem J* 297:595–601.
32. Beaven MA, *et al*. (1984) The mechanism of the calcium signal and correlation with histamine release in 2H3 cells. *J Biol Chem* 259:7129–7136.
33. Warner JA, MacGlashan DW, Jr (1990) Signal transduction events in human basophils. A comparative study of the role of protein kinase C in basophils activated by anti-IgE antibody and formyl-methionyl-leucyl-phenylalanine. *J Immunol* 145:1897–1905.
34. Parekh AB, Penner R (1995) Depletion-activated calcium current is inhibited by protein kinase in RBL-2H3 cells. *Proc Natl Acad Sci USA* 92:7907–7911.
35. Demaurex N, Orlowski J, Brisseau G, Woodside M, Grinstein S (1995) The mammalian Na^+/H^+ antiporters NHE-1, NHE-2, and NHE-3 are electroneutral and voltage independent, but can couple to an H^+ conductance. *J Gen Physiol* 106:85–111.
36. Sakai H, *et al*. (2006) pH dependence and inhibition by extracellular calcium of proton currents via plasmalemmal vacuolar-type H^+-ATPase in murine osteoclasts. *J Physiol* 576:417–425.
37. Plager DA, *et al.* (1999) A novel and highly divergent homolog of human eosinophil granule major basic protein. *J Biol Chem* 274:14464–14473.
38. Grinstein S, Romanek R, Rotstein OD (1994) Method for manipulation of cytosolic pH in cells clamped in the whole cell or perforated-patch configurations. *Am J Physiol* 267:C1152–C1159.
39. Siraganian RP (1974) An automated continuous-flow system for the extraction and fluorometric analysis of histamine. *Anal Biochem* 57:383–394.